Kinetic Manifestation of Processivity during Multiple Methylations Catalyzed by SET Domain Protein Methyltransferases†

Lynnette M. A. Dirk,‡ E. Megan Flynn,‡,§ Kevin Dietzel,‡,|| Jean-François Couture,⊥ Raymond C. Trievel,⊥ and Robert L. Houtz*,‡

Department of Horticulture, Plant Physiology/Biochemistry/Molecular Biology Program, 401D Plant Science Building, University of Kentucky, Lexington, Kentucky 40546-0312, and Department of Biological Chemistry, 5301 Medical Science Research Building III, University of Michigan Medical School, Ann Arbor, Michigan 48109-0606

Received November 15, 2006; Revised Manuscript Received January 12, 2007

ABSTRACT: Processive versus distributive methyl group transfer was assessed for pea Rubisco large subunit methyltransferase, a SET domain protein lysine methyltransferase catalyzing the formation of trimethyllysine-14 in the large subunit of Rubisco. Catalytically competent complexes between an immobilized form of des(methyl) Rubisco and Rubisco large subunit methyltransferase were used to demonstrate enzyme release that was co-incident with and dependent on formation of trimethyllysine. Catalytic rate constants determined for formation of trimethyllysine were considerably lower (∼10-fold) than rate constants determined for total radiolabel incorporation from [^{3}H-*methyl*]-*S*-adenosylmethionine. Double-reciprocal velocity plots under catalytic conditions favoring monomethyllysine indicated a random or ordered reaction mechanism, while conditions favoring trimethyllysine suggested a hybrid ping-pong mechanism. These results were compared with double-reciprocal velocity plots and product analyses obtained for *Hs*SET7/9 (a monomethyltransferase) and *Sp*CLR4 (a dimethyltransferase) and suggest a predictive ability of double-reciprocal velocity plots for single versus multiple methyl group transfers by SET domain protein lysine methyltransferases. A model is proposed for SET domain protein lysine methyltransferases in which initial binding of polypeptide substrate and *S*-adenosylmethionine is random, with polypeptide binding followed by deprotonation of the ϵ-amine of the target lysyl residue and subsequent methylation. Following methyl group transfer, *S*-adenosylhomocysteine and monomethylated polypeptide dissociate from monomethyltransferases, but di- and trimethyltransferases begin a successive and catalytically obligatory deprotonation of enzyme-bound methylated lysyl intermediates, which along with binding and release of *S*-adenosylmethionine and *S*-adenosylhomocysteine is manifested as a hybrid ping-pong-like reaction mechanism.

SET[1] [SU(VAR)3−9, E(Z), and TRX] domain protein lysine methyltransferases (PKMTs) catalyze the methylation of the ϵ-amine of specific lysyl residues in target protein substrates and appear to be ubiquitous across all eukaryotic phyla (*1*). The diversity of SET domain PKMTs is reflected by the occurrence of methylated lysyl residues in a number of essential but unrelated proteins (*2*). Recently, this class of protein methyltransferases has received widespread attention as being influential in the epigenetic regulation of gene expression through methylation of histone lysyl residues, and the subsequent recruitment of chromatin-modifying and remodeling proteins (*3*−*5*). Site and product specificity are both determinants in the regulation of gene expression by histone-specific SET domain PKMTs (*6*). Thus, these enzymes have been described with specificity for particular lysyl residues as well as in the number of methyl groups transferred (*7*). However, all SET domain PKMTs have a unique and conserved structural motif that contains separate binding sites for the target protein substrate and the methyl donor, *S*-adenosylmethionine (AdoMet) (*4*). The geometric arrangement of substrate binding sites on opposite sides of SET domain PKMTs, connected by a narrow channel through which methyl group transfer occurs, has been described as being ideal for the multiple transfer of methyl groups without dissociation of the protein substrate (*8*). Multiple methyla-

† This work was supported by Department of Energy Grant DE-FG02-92ER20075 to R.L.H. and National Institutes of Health Grant GM073839 to R.C.T. J.-F.C. is a Canadian Institutes of Health Research Postdoctoral Fellow.

* To whom correspondence should be addressed: Department of Horticulture, Plant Physiology/Biochemistry/Molecular Biology Program, 401D Plant Science Bldg., University of Kentucky, Lexington, KY 40546-0312. Telephone: (859) 257-1982. Fax: (859) 257-7874. E-mail: rhoutz@uky.edu.

‡ University of Kentucky.

§ Current address: Department of Molecular and Cellular Biology, University of California, Berkeley, CA 94720.

|| Current address: Microbiology Graduate Student, University of California, Davis, CA 95616.

⊥ University of Michigan Medical School.

[1] Abbreviations: SET, founding members of the domain SU(VAR)3−9, E(Z), and TRX; Rubisco, ribulose-1,5-bisphosphate carboxylase/oxygenase; *Hs*SET7/9, *Homo sapiens* histone H3 lysine-4-specific SET7; *Sp*CLR4, *Schizosaccharomyces pombe* cryptic loci regulator 4; PKMT, protein lysine methyltransferase; AdoMet, *S*-adenosyl-L-methionine; MeLys, ϵ-*N*-monomethyllysine; Me_2Lys, ϵ-*N*-dimethyllysine; Me_3Lys, ϵ-*N*-trimethyllysine; AdoHcy, *S*-adenosylhomocysteine; MALDI-TOF, matrix-assisted laser desorption ionization time-of-flight; *Ps*LSMT, *Pisum sativum* large subunit of Rubisco methyltransferase; LS, large subunit; PVDF, polyvinylidene difluoride; TLC, thin layer chromatography.

10.1021/bi6023644 CCC: $37.00
Published on Web 03/06/2007

tions catalyzed by SET domain PKMTs can occur by processive or distributive mechanisms. These two possibilities should be accompanied by different kinetic reaction mechanisms and, moreover, specific stoichiometric requirements for product formation. Distributive formation of a polypeptide-bound trimethyllysyl (Me_3Lys) residue would result in the intermediate formation and release of polypeptides with monomethyllysyl (MeLys) and dimethyllysyl (Me_2Lys) residues as reaction products which could exceed the active site concentration of the methyltransferase, while processive formation would restrict the stoichiometry of MeLys and Me_2Lys residues as reaction intermediates with cumulative amounts equal to or less than the total enzyme active site density. The kinetic reaction mechanisms would also be expected to be entirely different for these two models. A distributive mechanism with the release of partially methylated products should exhibit random or ordered bi-bi reaction kinetics, albeit with some considerations accommodating the binding and release of alternative substrates, i.e., partially methylated products. A processive mechanism, however, involves the repetitive binding and release of AdoMet and *S*-adenosylhomocysteine (AdoHcy) from an enzyme complex containing nonmethylated as well as methylated reaction intermediates. The closest approximation to this type of reaction mechanism is a ping-pong system in which the complex of the methyltransferase and each of the methylated intermediates can be considered as a modified form of the enzyme. Previous reports have described both processive (*9*−*11*) and distributive (*12*, *13*) mechanisms for SET domain PKMTs. However, an important criterion for determining kinetic reaction mechanisms is sufficient time for catalytic turnover and product formation during enzyme assays, accompanied by quantitative product analyses. While this is not a concern for most enzymes, SET domain PKMTs may be an exception. First, these enzymes have extremely low k_{cat} values ranging from 0.004 to 0.1 s^{-1}, typically determined by the incorporation of radiolabel from [^{3}H-*methyl*]AdoMet into synthetic or native polypeptide substrates. Because radiolabel incorporation does not distinguish between single and multiple methyl group transfers, the currently reported k_{cat} values for SET domain PKMTs, with the exception of monomethyltransferases, may or may not be representative of turnover rates for final product formation. Additionally, matrix-assisted laser desorption ionization time-of-flight (MALDI-TOF) mass spectroscopy is frequently used to assess product formation by the relative distribution of mass increases associated with the formation of methylated lysines over time, but this technique is usually qualitative unless multiple internal standards are part of each quantification (*14*, *15*). Thus, assignment of distributive versus processive methylation using such methods may be ambiguous.

*Ps*LSMT is the pea (*Pisum sativum*) SET domain nonhistone PKMT responsible for the formation of Me_3Lys-14 in the large subunit (LS) of Rubisco and was originally purified to homogeneity (~7000-fold) using an affinity purification technique that relied on tight and specific binding to PVDF-immobilized des(methyl) Rubisco (*16*). Previous studies demonstrated that release of *Ps*LSMT from immobilized Rubisco is a function of catalytic activity and subsequent methylation of bound Rubisco (*16*). In this report, we utilized the tight and specific binding of *Ps*LSMT to immobilized Rubisco and the dependency on catalytic methylation for the release of the enzyme to determine whether this enzyme's multiple methylations are processive or distributive in nature. Additionally, we utilized this information to conduct a double-reciprocal velocity plot analysis for *Ps*LSMT, as well as two other SET domain histone PKMTs, under conditions which resulted in defined product formation to elucidate the effect of multiple versus single methylation events on the appearance of kinetic reaction mechanism plots.

EXPERIMENTAL PROCEDURES

*Enzymes, Substrates, and Chemicals. Hs*SET7/9 (residues 1−366, 42.4 kDa), *Sp*CLR4 (residues 192−490, 34.2 kDa), and *Ps*LSMT (residues 38−485, 51.7 kDa) were expressed and purified as previously described (*8*, *17*, *18*). All enzymes were judged to be greater than 95% homogeneous as determined by SDS−PAGE. Calf thymus histone H3 was from Roche Diagnostics Corp. (Indianapolis, IN) and des(methyl) Rubisco purified from spinach (*19*). *S*-Adenosyl-L-methionine (AdoMet) from Sigma was purified prior to use as described previously (*20*). [^{3}H-*methyl*]AdoMet (~70−80 Ci/mmol) was from GE Healthcare (formerly Amersham Biosciences Corp., Piscataway, NJ) and diluted to a specific activity of 1−4 μCi/nmol for enzyme assays. Immobilon-P (PVDF) membrane was from Millipore (Bedford, MA). All other chemicals and reagents were from Sigma or Bachem.

Methyltransferase Assays. Previously described enzyme assays (*8*, *21*) were optimized for linearity with time and enzyme concentration. Substrate consumption was limited to ≤20%, and assays were optimized to support single or multiple turnovers based on k_{cat} values determined by preliminary experiments that documented Me_2Lys or Me_3Lys product formation, respectively. In general, assays were conducted in a total volume of 20 μL except where conditions were modified to support the aforementioned optimization parameters which necessitated volumes as large as 100 μL. Calf thymus histone H3 was used as the polypeptide substrate for *Hs*SET7/9 and *Sp*CLR4 and purified spinach Rubisco for *Ps*LSMT. Enzyme concentrations were 1.6 μM for *Hs*SET7/9, 1.5 μM for *Sp*CLR4, and 6.4 nM to 3.9 μM for *Ps*LSMT.

Association of PsLSMT with PVDF-Immobilized Des(methyl) Rubisco and Scatchard Plot Analyses. PVDF disks (0.4−0.6 cm in diameter) were saturated with des(methyl) spinach Rubisco as previously described (*16*) and incubated with 500 nM *Ps*LSMT in a final volume of 800 μL, and aliquots were removed with time and assayed for *Ps*LSMT activity for determination of association with immobilized Rubisco. Similar conditions were used for determination of the binding affinity between *Ps*LSMT and Rubisco, except two disks in 0.8 mL were incubated for 5−6 h at ~25 °C with varying concentrations of *Ps*LSMT (from 20 to 3000 nM). After equilibrium had been reached, samples were removed for determination of the amount of *Ps*LSMT remaining in solution (free), and the amount of bound *Ps*LSMT was calculated (*16*). The data were plotted and analyzed.

Catalytic Release of PsLSMT from PVDF-Immobilized Rubisco and Product Analyses. One PVDF disk, saturated with des(methyl) Rubisco and with bound *Ps*LSMT (4.3 μg,

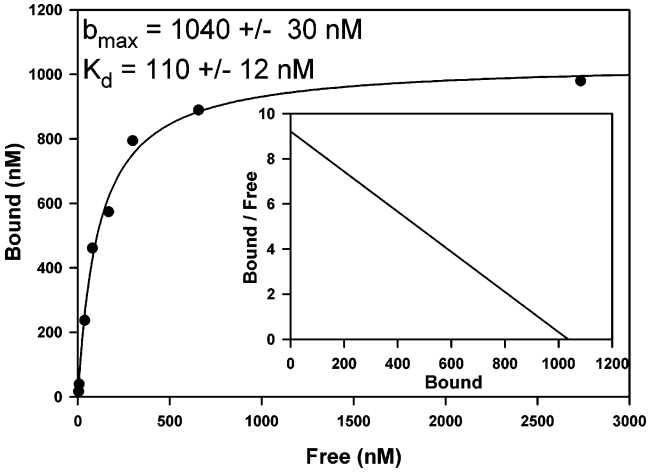

FIGURE 1: Binding affinity between *Ps*LSMT and immobilized des(methyl) Rubisco. PVDF disks were saturated with purified spinach Rubisco and subsequently incubated for 5−6 h at ~22 °C with concentrations of *Ps*LSMT in the 20−3000 nM range as described in Experimental Procedures. The data were plotted and analyzed. The inset is a Scatchard plot. b_{max} is the total number of *Ps*LSMT binding sites and K_d the *Ps*LSMT dissociation constant.

83.3 pmol), was inserted into a 70 μL drop [elution solution consisting of 100 mM Bicine (pH 8.0), 0.5 mg/mL β-lactoglobulin, 2 mM $MgCl_2$, and 100 μM [^{3}H-*methyl*]AdoMet (~1 μCi/nmol)] placed on a square (~2 cm × 2 cm) of Parafilm M barrier film (SPI Supplies and Structures Probe Inc., West Chester, PA). The fastidiously timed reaction was terminated by removing the disk from the elution solution and immediately immersing the disk in a terminating solution [consisting of 250 μL of 100 mM Mes (pH 6.0), 150 mM NaCl, and 1 mM AdoHcy]. *Ps*LSMT was completely inhibited under these conditions; therefore, the distribution of MeLys, Me_2Lys, and Me_3Lys as products was preserved on the disks. Aliquots of the elution solutions (18 μL) were analyzed for *Ps*LSMT activity in assessing the release of *Ps*LSMT from PVDF-immobilized Rubisco by addition of a saturating amount of Rubisco (~0.5 mg) and incubation at 30 °C for 4 min and processing as described previously (*16*). Inhibition by AdoHcy was minimized by diluting the elution 5-fold and using 100 μM AdoMet in the assay. Simultaneously, disks were washed five times each with terminating solution (250 μL). The disk from each time point was subjected to acid hydrolysis (6 N HCl at 110 °C for 22 h) in vacuum hydrolysis tubes (Pierce Biotechnology Inc., Rockford, IL). After hydrolysis, the samples were evaporated to dryness, the residue was dissolved in 15 μL of 100 mM bicine (pH 8.2) (three 5 μL aliquots), Lys, MeLys, Me_2Lys, and Me_3Lys standards were added, and the samples were applied to thin layer chromatography (TLC) plates (*22*). R_f regions corresponding to methylated lysine derivatives were removed, and analysis of radiolabel incorporation was conducted by liquid scintillation spectroscopy. Experiments were conducted at 22 and 4 °C.

RESULTS

*Ps*LSMT binds tightly to PVDF-immobilized des(methyl) forms of Rubisco (Figure 1). The $t_{1/2}$ for dissociation of bound Rubisco LSMT from immobilized Rubisco is 192 h, and thus, the complex is stable; within the time frame of the following studies, spontaneous dissociation of *Ps*LSMT essentially does not occur (*2*). These conditions provided a unique opportunity to directly assess the dissociation of *Ps*LSMT from Rubisco as a function of methylation at Lys-14. Within the context of catalytic turnover events, dissociation after MeLys, Me_2Lys, or Me_3Lys should result in (1) a methylation "footprint" at Lys-14, discernible after complete acid hydrolysis of immobilized Rubisco followed by quantitative analyses of incorporation of [^{3}H]methyl into methylated lysyl derivatives, and (2) co-incident dissociation of *Ps*LSMT into solution, which can be quantified by enzymatic activity measurements. Thus, unequivocal evidence for a processive mechanism or a distributive mechanism for methyl group transfer should be obtained. Preliminary experiments demonstrated complete release of bound *Ps*LSMT after extended incubation with AdoMet, as previously reported for purification of native *Ps*LSMT (*16*). In the presence of saturating levels of [^{3}H-*methyl*]AdoMet at 22 °C, the immobilized *Ps*LSMT−Rubisco complex rapidly incorporated [^{3}H]methyl groups into MeLys, Me_2Lys, and Me_3Lys which were separated and individually quantified. During the initial 20 s of the reaction, MeLys was the major product at 25 pmol, representing 30% of the total molar mass of bound *Ps*LSMT (~83.3 pmol) (Figure 2, lower axes). Roughly equal but smaller amounts of Me_2Lys and Me_3Lys (~10 pmol) were observed during this same time, both of which approximated the level of soluble dissociated *Ps*LSMT (Figure 2, lower axes). Individual rate constants calculated for formation of Me-, Me_2-, and Me_3Lys from the unmethylated substrate were 0.02, 0.0052, and 0.0046 s^{-1}, respectively. Thus, the initial formation of MeLys was nearly 4-fold faster than subsequent methylations, and the rate constant for formation of Me_3Lys was only 9.2% of the reported k_{cat} of 0.05 s^{-1} measured using total incorporation of the radiolabel from [^{3}H-*methyl*]AdoMet (*8*, *21*); however, after 20 s, both MeLys and Me_2Lys fell to steady state levels of approximately 20 and 10 pmol, respectively, for the remaining 110 s of the experiment. Therefore, under steady state conditions, the rate constants for formation of MeLys, Me_2Lys, and Me_3Lys must be equal, and the rate constant for MeLys formation was reduced approximately 4-fold, from the initial value of 0.02 s^{-1} to the rate for Me_3Lys, 0.0046 s^{-1}. Only the level of Me_3Lys continued to increase in a linear, 1:1 fashion co-incident with an increasing release of *Ps*LSMT into solution (Figure 3). The profiles for MeLys and Me_2Lys formation were as expected for intermediates between lysine and the formation of Me_3Lys, and their combined amounts never exceeded the total active site density of *Ps*LSMT, characteristic of a processive reaction mechanism. The stoichiometries were corroborated by the observation that the total mass of soluble *Ps*LSMT plus bound *Ps*LSMT, the latter estimated by the intermediate steady state levels of MeLys and Me_2Lys at 130 s, was approximately 84% of the starting total mass of *Ps*LSMT bound to immobilized Rubisco (83.3 pmol). Although the initial pre-steady state reaction rates for methylated lysyl derivatives were substantially lower than the reported k_{cat} of 0.05 s^{-1} for *Ps*LSMT, if these values were transformed to reflect incorporation of the radiolabel from [^{3}H-*methyl*]-AdoMet (2× for Me_2Lys and 3× for Me_3Lys), the overall rate constant became 0.04 s^{-1} (80% of 0.05 s^{-1}). Similarly, under steady state conditions where the reaction rates were equal for MeLys, Me_2Lys, and Me_3Lys at 0.0046 s^{-1},

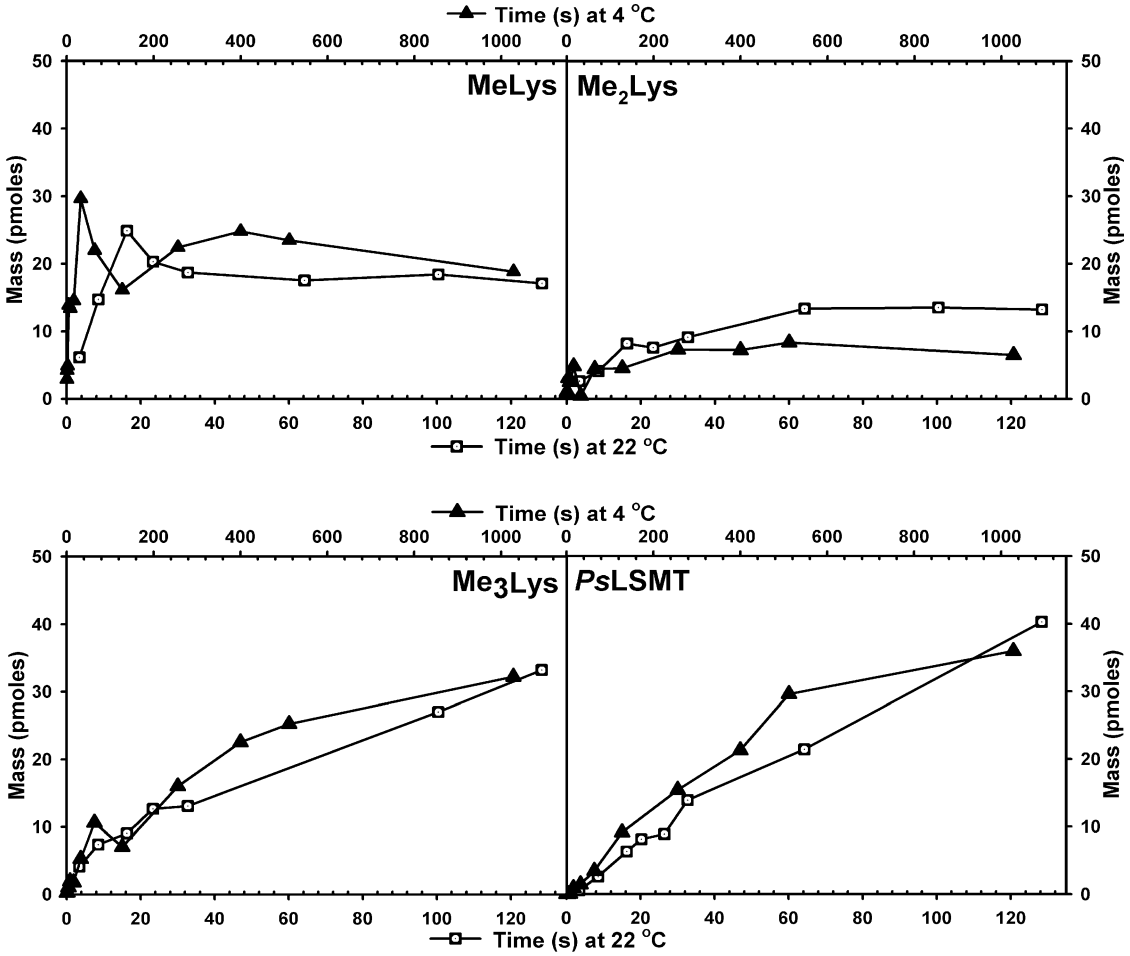

FIGURE 2: Rubisco LS Lys-14 methylation and catalytic-dependent dissociation of *Ps*LSMT into solution. After measured times under catalytic conditions at either 4 (upper axes) or 22 °C (lower axes) in the presence of [^{3}H-*methyl*]AdoMet, PVDF disks were analyzed for Me-, Me_2-, and Me_3Lys, and the elution solution was analyzed for *Ps*LSMT release (~83.3 pmol bound at the start) as described in Experimental Procedures.

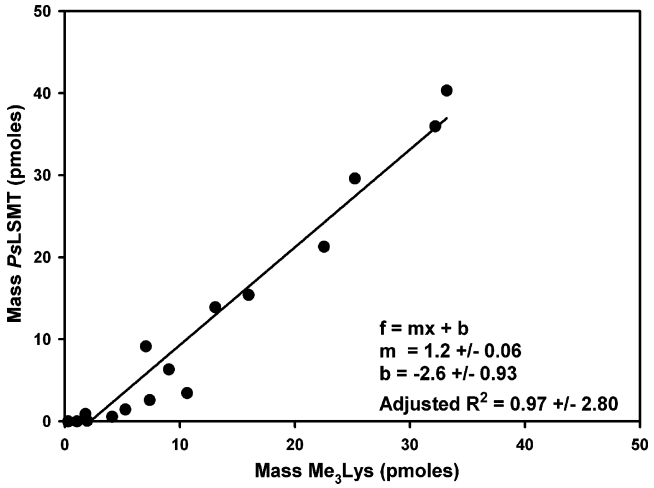

FIGURE 3: Linear regression analysis of Me_3Lys formation and *Ps*LSMT dissociation. The mass of *Ps*LSMT released during catalysis as described in Figure 2 plotted against the mass of Me_3Lys formed during that same time was fitted with a linear equation.

the linear loss of bound *Ps*LSMT (~52% remaining at 130 s) translates to a combined rate constant for total radiolabel incorporation at 130 s of 0.0552 s^{-1}. Therefore, the immobilized complex between *Ps*LSMT and Rubisco exhibited catalytic activity which approximates that determined in solution with saturating substrates and supported the relevance of the immobilized complex for product analyses.

In an effort to slow catalytic turnover and perhaps gain a more defined relationship between product formation and *Ps*LSMT release, the experiment was repeated at 4 °C (Figure 2, upper axes). Preliminary experiments were used to define appropriate times for sufficient product formation and reliable detection. Aside from the slower rate constants for product formation, the results were identical with those obtained at 22 °C (Figure 2, triangles vs squares). After an initial rapid increase in the formation of MeLys, during which there was little release of *Ps*LSMT, the amount of MeLys declined to a steady state level of approximately 20 pmol. The profiles for formation of Me_2Lys and Me_3Lys were also similar with a steady state level of ~10 pmol for Me_2Lys and a direct 1:1 relationship between formation of Me_3Lys and detection of soluble *Ps*LSMT activity (Figure 3). These results again strongly suggested an intermediate type of relationship for MeLys and Me_2Lys in the reaction from lysine to Me_3Lys catalyzed by *Ps*LSMT and a processive mechanism in which *Ps*LSMT did not dissociate from Rubisco after formation of MeLys or Me_2Lys. When the molar stoichiometries between *Ps*LSMT release and formation of Me_3Lys from Figure 2 were combined, a significant 1:1 linear relationship was evident (Figure 3, slope of ~1.0),

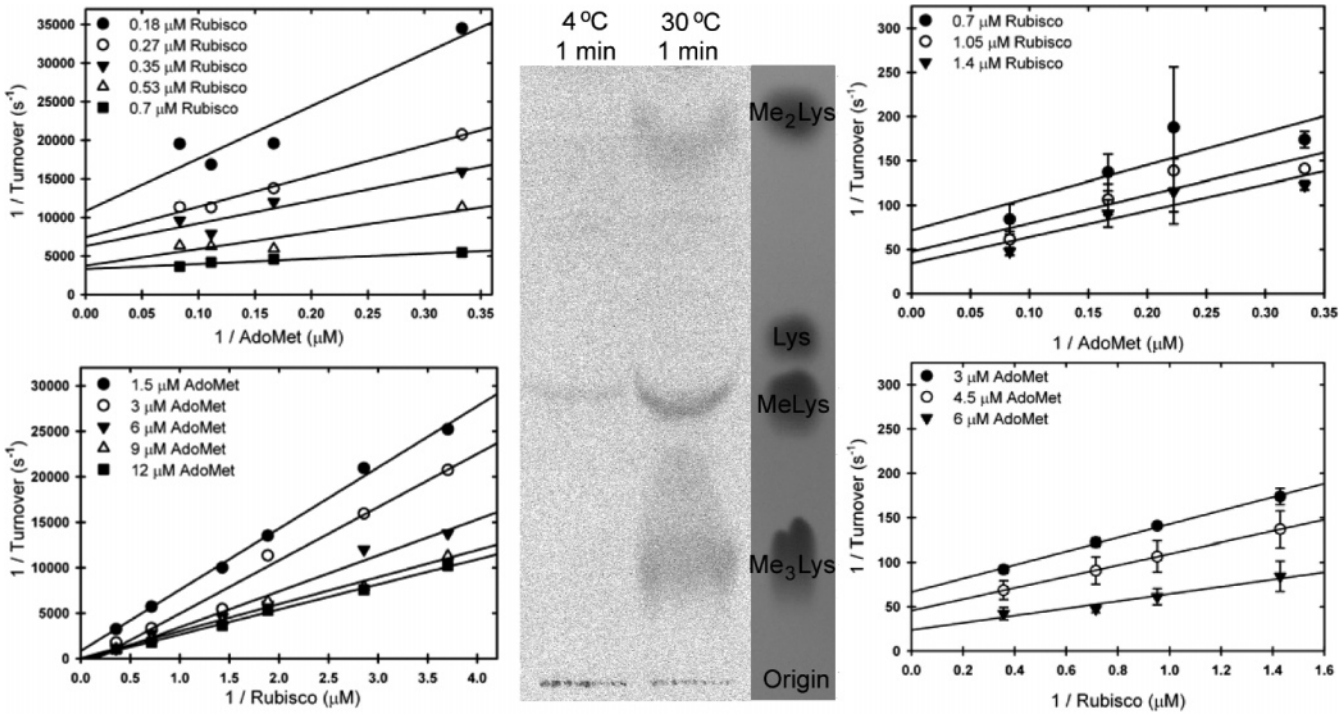

FIGURE 4: Product distribution (1 min) and kinetic analyses (various times) of *Ps*LSMT under conditions limiting product to MeLys (4 °C) or maximizing Me_3Lys formation (30 °C). Phosphorimage analysis of silica gel TLC of acid hydrolysate (middle) from assays with either large amounts of *Ps*LSMT and substrate at a low temperature (4 °C) or a limiting amount of enzyme at the optimal temperature (30 °C), as described in Experimental Procedures. An image of the ninhydrin-developed TLC plate with labeling of the Lys standard and its methylated derivatives was provided for comparison. Double-reciprocal plots for Rubisco and AdoMet of *Ps*LSMT under conditions which limit product to MeLys (left half). Incorporation of the radiolabel from [^{3}H-*methyl*]AdoMet into base-stable protein precipitates was assessed from methyltransferase assays conducted for 1 min with 4 μg of enzyme at 4 °C, which restricted product formation to MeLys-14. Turnovers were calculated, and the double-reciprocal plots were plotted. The kinetic constants derived from the replots of the slopes from the double-reciprocal plots were determined to be 0.002 s^{-1}, 2.7 and 3.9 μM for AdoMet and Rubisco, respectively. K_m values are within 3-fold of previously published constants for *Ps*LSMT (*8*). Double-reciprocal plots for Rubisco and AdoMet of *Ps*LSMT under conditions which maximize Me_3Lys product formation (right half). Activity assays were conducted with a limiting amount of enzyme (33 ng of *Ps*LSMT) in larger assay volumes (100 μL) for various protracted times at 30 °C to increase the level of Me_3Lys formation. The kinetic constants derived from the replots of the slopes from the double-reciprocal plots were determined to be 0.073 s^{-1}, 7.5 and 1.7 μM for AdoMet and Rubisco, respectively. These are within 2-fold of previously published constants for *Ps*LSMT (*8*).

but not with Me- or Me_2Lys (slope of ~0.2 for both, data not shown).

A processive mechanism for methyl group transfer has interesting mechanistic and kinetic implications. Mechanistically, the intermediates formed between *Ps*LSMT and methylated lysyl derivatives do not dissociate during catalysis, and our observations support this model. Thus, partially methylated substrates might not faithfully mimic conformations that may exist in the enzyme-bound forms of MeLys and Me_2Lys intermediates, and inferences deduced with regard to reaction mechanisms and catalytic competency may be invalid using partially methylated substrates. Kinetically, the enzyme−intermediate complexes formed between *Ps*LSMT and Rubisco with MeLys and Me_2Lys-14 were similar to enzyme intermediates in a ping-pong reaction mechanism with successive binding and release of AdoMet and AdoHcy. However, given the slow turnover for final product formation (Me_3Lys, 0.0046 s^{-1}; see above), an analysis of the kinetic reaction mechanism using rate constants derived from incorporation of radiolabel from [^{3}H-*methyl*]AdoMet alone (i.e., in the absence of product analysis) could be misleading. Complete catalytic turnover and product formation, such as Me_3Lys formation, required a minimum of 217 s rather than the 20 s estimated from total [^{3}H-*methyl*]AdoMet incorporation. Therefore, under saturating conditions, Me_3Lys formation would necessitate a 217 s minimal assay time, whereas kinetic analyses of the *Ps*LSMT reaction mechanism, conducted under conditions with less than saturating substrates, require further increases in assay times. We compared double-reciprocal velocity plot determinations for *Ps*LSMT under catalytic conditions which supported the formation of either MeLys or Me_3Lys on the basis of the previous studies. Short reaction times (1 min) at 4 °C followed by product analyses demonstrated that MeLys was essentially the only product, while reactions at 30 °C for 1 min favored Me_3Lys formation (Figure 4). Double-reciprocal velocity plots of Rubisco LSMT turnover rates versus concentration of AdoMet or Rubisco at varying concentrations of Rubisco or AdoMet at 4 °C resulted in the formation of a family of intersecting lines (Figure 4, left half). Double-reciprocal velocity plots of enzyme activity that yield intersecting lines are indicative of either a random or an ordered bi-bi reaction mechanism, consistent with this bisubstrate system. However, identical analyses under conditions that strongly favor catalytic formation of Me_3Lys (30 °C, assays for ≥10 min) resulted in double-reciprocal velocity plots which were instead shifted to a family of parallel lines (Figure 4, right half). A set of parallel lines is frequently associated with a ping-pong kinetic reaction mechanism, wherein the binding of the first substrate results in the formation of an enzyme-bound intermediate with product release prior to the binding of the second substrate and final product formation.

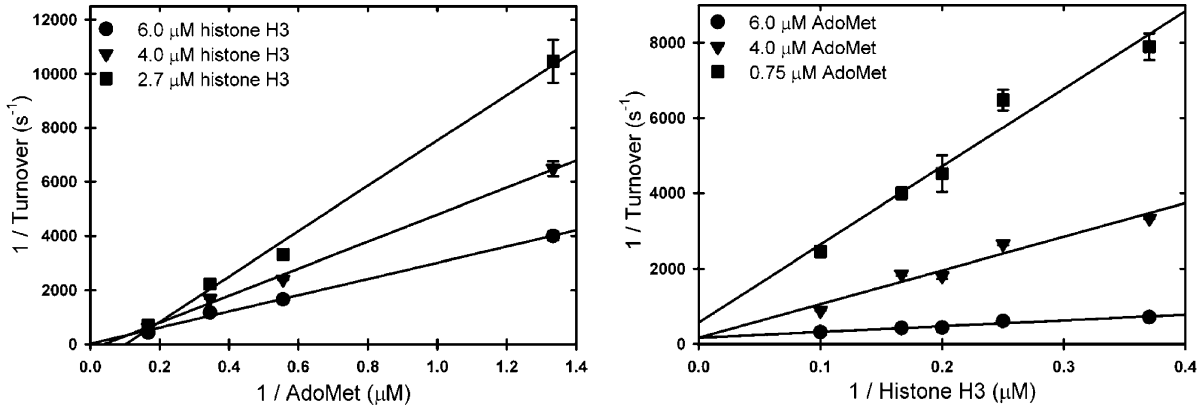

FIGURE 5: Double-reciprocal plots for calf thymus histone H3 and AdoMet of *Hs*SET7/9. The kinetic constants derived from the replots of the slopes from the double-reciprocal plots were determined to be 0.012 s^{-1}, 3.5 and 28 μM for AdoMet and calf thymus histone H3, respectively. These are within 5-fold of previously published constants for *Hs*SET7/9 (*8*).

Assessing dissociation of enzyme from an enzyme−polypeptide substrate complex for other SET domain PKMTs, as demonstrated in Figures 2 and 3 for *Ps*LSMT and Rubisco, may not be easy. We considered, however, that double-reciprocal velocity plot analyses, as well as supporting evidence provided by product distribution analyses, performed under identical conditions, might be an experimental technique capable of providing evidence of processive versus distributive methyl group additions in other PKMTs. Therefore, we examined the double-reciprocal velocity plots for *Hs*SET7/9 and *Sp*CLR4, histone H3 Lys-4- and Lys-9-specific PKMTs, respectively, and compared the results predicted by the velocity plots and product distribution analyses (single vs multiple methylations and processive vs distributive methyl group transfer) with the data obtained for *Ps*LSMT.

The family of lines in the double-reciprocal velocity plots for *Hs*SET7/9 using histone H3 as the polypeptide substrate under conditions supporting multiple catalytic turnovers intersected near the origin (Figure 5). The only product under the same conditions used for kinetic reaction mechanism analyses was MeLys (data not shown), correlating with previous studies of the product specificity of this PKMT (*11*, *23*). Thus, taken together, these findings confirmed *Hs*SET7/9 as a monomethyltransferase with either an ordered or random bi-bi reaction mechanism. Similar analyses for *Sp*CLR4, however, demonstrated a family of parallel lines indicative of multiple methylations, which was confirmed by product analyses that showed the presence of Me_2Lys as the predominant product from *Sp*CLR4-catalyzed methylation of histone H3 (Figure 6). We were unable to identify assay conditions for *Sp*CLR4 which maintained linearity beyond 2 min. Nevertheless, the data obtained with formation of Me_2-Lys clearly suggest a hybrid ping-pong like reaction mechanism for *Sp*CLR4. Under extended assay conditions, a small amount of Me_3Lys can be detected as a product of *Sp*CLR4 activity (data not shown, but see also Figure 6). These results suggest that *Sp*CLR4 is a processive enzyme during the catalytic formation of Me_2Lys, and possibly Me_3Lys as well.

A processive mechanism for methyl group transfer by SET domain PKMTs like *Ps*LSMT necessitates removal of the proton from the ϵ-amine of bound target lysyl residues and implicitly suggests a mechanism for proton abstraction within the active site. Residues within the active site positioned for proton abstraction are unlikely to exist (*4*, *17*, *23*, *24*), which along with the distinctly alkaline pH optima for the k_{cat} of many SET domain PKMTs, including *Ps*LSMT (*25*), DIM-5 (*11*), *Hs*SUV39H1 (*13*), *Paramecium bursaria* chlorella virus 1 [PBCV-1 (*24*)], and *Hs*SET7/9 (*8*), have prompted proposals that SET domain PKMTs may preferentially bind the unprotonated form of the target lysyl residue. The active site of *Ps*LSMT is devoid of ionizable residues that could act as general bases. However, increasing turnover rates with increasing pH could be a consequence of changes in the relative distribution of protonated versus unprotonated target lysyl residues as well as differences in the binding affinities by SET domain PKMTs for target lysyl residues in the protonated versus unprotonated states. Therefore, we examined the effect of pH on the k_{cat} and K_m values for AdoMet and histone H3 by *Hs*SET7/9 (Figure 7). Although there was a 7-fold increase in k_{cat} with an increase in pH from 7.5 to 9.5, similar to that reported previously (*8*), this was not accompanied by changes in enzyme affinity for AdoMet or, more importantly, histone H3. At lower pH values, the relative changes in protonated versus unprotonated target lysyl residues would admittedly be small (assuming a pK_a of ~10); however, across the entire pH range examined in these studies from 7.5 to 9.5, the relative distribution would change by 100-fold, and at pH 9.5, ~32% of the target lysyl residue would be deprotonated. Thus, there was a distinct and significant increase in enzyme efficiency for *Hs*SET7/9 with an increase in pH, which along with the absence of any changes in binding affinity for histone H3 suggests that there is not a preference for unprotonated versus protonated target lysyl residues and that the effect of pH on turnover must be mediated within the active site of *Hs*SET7/9 and presumably other SET domain PKMTs.

DISCUSSION

Utilizing successive methyl group additions without dissociation from Rubisco, *Ps*LSMT catalyzes the trimethylation of lysyl residue 14 in the LS of Rubisco by a processive mechanism. Direct measurements of dissociation of *Ps*LSMT from immobilized Rubisco as a function of the extent of MeLys, Me_2Lys, or Me_3Lys-14 formation demonstrate that *Ps*LSMT dissociation occurs only after formation of Me_3Lys. Distribution analyses of modified lysyl residues formed under pre-steady state conditions would theoretically provide evidence of turnover rates specific for MeLys, Me_2-Lys, and Me_3Lys, all of which were considerably lower than

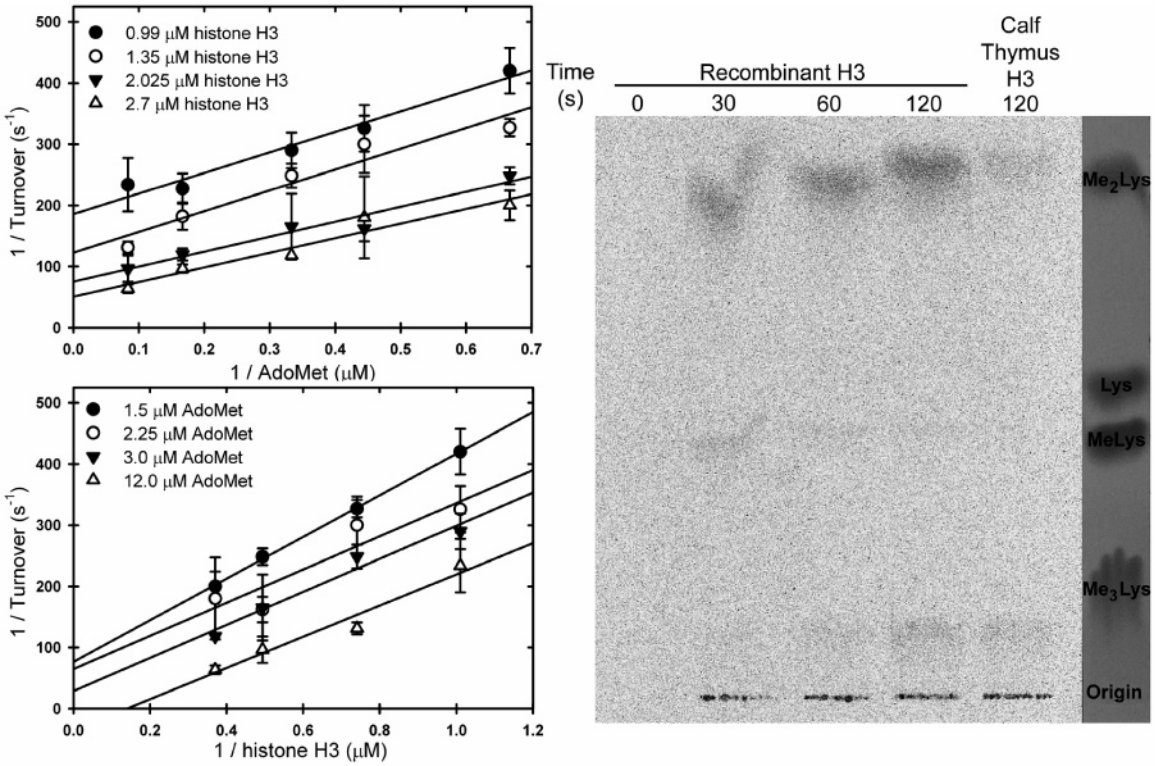

FIGURE 6: Double-reciprocal plots for calf thymus histone H3 and AdoMet of *Sp*CLR4. The kinetic constants derived from the replots of the slopes from the double-reciprocal plots were determined to be 0.073 s^{-1}, 31 and 15 μM for AdoMet and calf thymus histone H3, respectively. These values are within 7-fold of previously published constants for *Sp*CLR4 which used a 15-residue histone H3 substrate peptide (*18*). Phosphorimage analysis of silica gel TLC of acid hydrolysate of *Sp*CLR4 assays with recombinant histone H3 as a function of time was compared with that for assay conditions used for kinetic analyses. An image of the ninhydrin-developed TLC plate labeled according to the position of Lys and its methylated derivatives was aligned at the right.

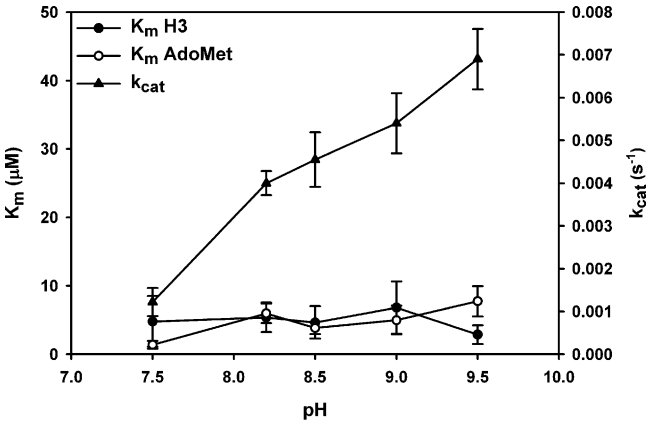

FIGURE 7: Turnover and apparent affinities of *Hs*SET7/9 for calf thymus histone H3 and AdoMet as a function of pH. Bicine was adjusted to each of the five pH values, and saturating assays were used to derive a Michaelis−Menten equation for both substrates. The apparent K_m values from these curves were then plotted as a function of pH.

the overall rate constant for incorporation of radiolabel from [^{3}H-*methyl*]AdoMet. The profile of mass changes in MeLys and Me_2Lys under steady state conditions remained constant, never cumulatively exceeding the active site density of *Ps*LSMT, confirming their role as intermediates in the formation of Me_3Lys and not products per se. This report is the only kinetic study of a SET domain PKMT catalyzing multiple methylations using an intact polypeptide substrate and quantitative product analyses under pre-steady and steady state conditions. The lack of dissociation of *Ps*LSMT from Rubisco during formation of MeLys-14 and Me_2Lys-14 was further supported by double-reciprocal velocity plot analyses. Under assay conditions which support multiple catalytic turnovers and formation of Me_3Lys, double-reciprocal velocity plots indicated a hybrid ping-pong-like reaction mechanism. However, identical analyses performed under conditions that support only formation of MeLys-14 resulted instead in double-reciprocal velocity plots indicative of either an ordered or random bi-bi reaction mechanism. Similar analyses of *Hs*SET7/9 and *Sp*CLR4 under conditions supporting MeLys and Me_2Lys product formation, respectively, support a hybrid ping-pong-like reaction mechanism for multiple methyl group transfers but a random or ordered mechanism for monomethyltransferases like *Hs*SET7/9. Ping-pong reaction mechanisms usually involve the binding and release of substrate and product prior to formation of an enzyme-bound intermediate. For *Ps*LSMT, beginning with formation of an enzyme-bound complex with Rubisco, the successive binding and release of AdoMet and AdoHcy, and multiple methylation events, is likely responsible for the appearance of a hybrid ping-pong-like double-reciprocal velocity plot. These results also dramatically emphasize the necessity for accurate determination of rate constants for product formation in SET domain PKMTs catalyzing multiple methylations, as reflected by the completely different kinetic reaction mechanism results depending on the k_{cat} values that are used. Although the SET domain is structurally conserved, both distributive and processive mechanisms have been described for SET domain PKMT enzymes catalyzing multiple methyl group transfers (*9*−*13*). However, it seems unlikely that enzymes catalyzing essentially the

same reaction utilizing a highly conserved catalytic structural motif would utilize different kinetic reaction mechanisms for multiple methyl group additions. Much of the evidence of processive transfer of methyl groups comes from MALDI-TOF mass spectroscopy analyses of either unmethylated or partially methylated synthetic polypeptide substrates and subsequent observations of relative changes in ion intensity for molecular mass shifts according to methyl group additions over time. In the absence of internal standards, quantitative relationships between enzyme active site density and product formation may not be obvious (*14*, *15*). Detailed kinetic reaction mechanisms have been reported for two SET domain PKMTs, G9a, a murine histone H3 Lys-9 di/trimethyltransferase (*10*, *12*), and SUV39H1, a human histone H3 Lys-9 trimethyltransferase (*13*). These studies reported a random bi-bi reaction mechanism for both enzymes but a processive addition of methyl groups for G9a, and distributive for SUV39H1, which is evident in MALDI-TOF mass spectroscopy analyses as well as steady state dilution experiments. The k_{cat} reported for G9a (88 h^{-1} or 0.024 s^{-1}) and SUV39H1 (12 h^{-1} or 0.0033 s^{-1}) in these studies was determined using total incorporation of radiolabel from [^{3}H-*methyl*]AdoMet. If, as in the studies reported here, the specific k_{cat} for formation of Me_3Lys is substantially smaller, then the assay time required for formation of Me_3Lys would be much longer than the period of 3 (G9a) or 30 min (SUV39H1) used in these studies, and the observed kinetic reaction mechanism may have possibly appeared as a random or an ordered bi-bi mechanism rather than ping-pong. It is worth noting that the PKMT, cytochrome *c* lysine *N*-methyltransferase (Ctm1p), which catalyzes trimethylation of cytochrome *c*, has been extensively kinetically characterized as well as subjected to complete product analyses and quantification of MeLys, Me_2Lys, and Me_3Lys. The results from these studies provided evidence that MeLys and Me_2Lys were intermediates in the formation of Me_3Lys, and the authors concluded that there was a processive addition of methyl groups and the enzyme had a hybrid ping-pong reaction mechanism (*26*, *27*).

The significant differences in the binding affinities of *Ps*LSMT for Rubisco in the absence and presence of AdoMet (K_d = 110 nM vs K_m = 2.8 μM) suggest that there may be communication between the polypeptide and AdoMet binding sites in *Ps*LSMT. Previous studies have demonstrated ordering of the cSET region in response to AdoMet binding in PR-SET7 (*28*), as well as structural ordering of the post-SET domain in DIM5 in response to substrate binding (*11*), and participation of the C-terminal segment in substrate binding site formation in SET7/9 (*23*). Previous docking models have suggested an extensive interaction between *Ps*LSMT and Rubisco, potentially involving the C-terminal lobe region unique to *Ps*LSMT (*17*). The inability of Rubisco bearing Me_3Lys-14 to bind *Ps*LSMT with any appreciable affinity (*16*), and the observation of its dissociation as the final product from the *Ps*LSMT−Rubisco complex as demonstrated here, suggest that formation of Me_3Lys may result in extensive conformational changes in *Ps*LSMT which ultimately result in release from Rubisco. A requirement for a conformational change in *Ps*LSMT prior to product release may also be reflected in the lag between Me_3Lys formation and release of immobilized *Ps*LSMT.

For PKMTs catalyzing multiple methylations, formation of the polypeptide-bound MeLys intermediate creates a net positive charge on the ϵ-nitrogen, which in addition to presenting an electrostatically unfavorable active site environment for subsequent binding of AdoMet with its positively charged sulfonium group is also catalytically incompetent for an S_N2 nucleophilic transfer. The active site of *Ps*LSMT, as well as other SET domain PKMTs, has been examined for residues that could facilitate removal of a proton from the enzyme-bound target lysyl ϵ-nitrogen. Although Tyr-287 in *Ps*LSMT and the equivalent highly conserved active site Tyr residue in other SET domain enzymes were originally proposed as essential bases catalyzing proton removal, subsequent structural studies of ternary complexes of *Ps*LSMT, Lys, and MeLys clearly exclude this possibility (*17*). Thus, a solvent-catalyzed deprotonation event probably follows dissociation of AdoHcy prior to subsequent AdoMet binding and continued methylation, and numerous water molecules, found in the active site of many SET domain PKMTs, could well serve as proton acceptors and, thus, aid in the repositioning of the ϵ-nitrogen for further S_N2 reactions. Formation of Me_3Lys might be expected, however, to be catalytically favored under these circumstances, since the pK_a for Me_2Lys (10.0) is more than one-half unit below that for either lysine (10.6) or MeLys (10.7) (*29*). Instead, we observed that the pre-steady state rate constant for formation of MeLys exceeded the rate constants for Me_2Lys or Me_3-Lys. In addition to deprotonation, multiple methylations also necessitate considerable realignment of the ϵ-amine for subsequent methylations. Whether deprotonation precedes, follows, or is concomitant with ϵ-amine rearrangement is unknown, but perhaps the higher pre-steady state initial velocities observed for MeLys formation reflect the greater number of catalytically competent conformations available for an unmethylated ϵ-amine.

The observations and data presented here lead us to favor a model of SET domain PKMT activity which is, in the initial binding of AdoMet and polypeptide substrate, either ordered or random, followed by product release and completion of the reaction as in the case of monomethyltransferases (Figure 8c), but with multiple methyl group transfers, a requirement for additional deprotonation steps, and geometric ϵ-amine rearrangements involving enzyme-bound methylated lysyl intermediates prior to repetitive binding of AdoMet and release of AdoHcy that is manifested as a hybrid ping-pong-like reaction mechanism (Figure 8a,b). Previous kinetic analyses support random addition of substrates for G9a (*10*), and independent binding of AdoMet or Rubisco to *Ps*LSMT has also been demonstrated (refs *16* and *30* and this work). Certainly for multiple methyl group transfers by SET domain PKMTs, the reaction mechanism is not entirely a simple ping-pong mechanism, and it is notable there are circumstances for both ordered and random kinetic reaction mechanisms in which double-reciprocal velocity plots can be distorted to the extent of having the appearance of a ping-pong reaction mechanism. For example, ordered reaction mechanisms in which the initial association constant for the first substrate (K_{ia}) is considerably lower than the apparent K_m can have the appearances of a ping-pong reaction mechanism, and additionally, rapid equilibrium random mechanisms in which the rate constant for product release is considerably lower than the k_{cat} can also appear to be ping-

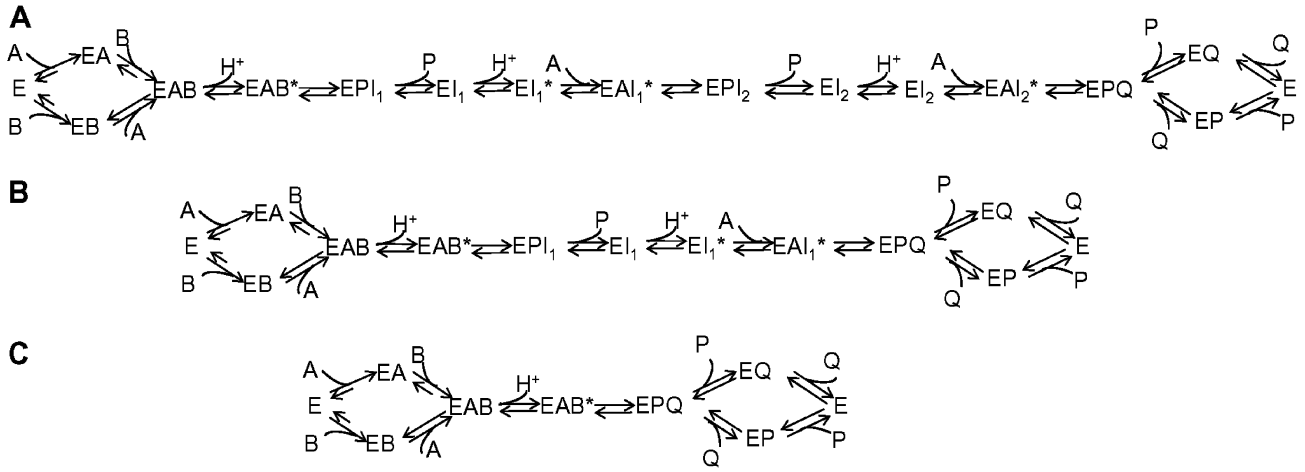

FIGURE 8: Generalized schemes of the reaction mechanism for tri- (A), di- (B), or monomethyltransferase (C) SET domain enzymes: E, SET domain enzyme; A, AdoMet; P, AdoHcy; B, polypeptide substrate; I_1, polypeptide substrate MeLys; I_2, polypeptide substrate Me_2Lys; Q, polypeptide substrate with the corresponding number of methyl groups given the number of methyl groups transferred by the given SET domain enzyme. An asterisk denotes a deprotonated form of a targeted Lys residue.

pong mechanisms (*31*). Indeed, the dissociation constant of *Ps*LSMT with des(methyl) Rubisco is approximately 10-fold lower than the K_m. However, the direct assessment of dissociation of *Ps*LSMT from Rubisco as a function of the level of Me_3Lys formation as in the studies presented here excludes a distributive reaction mechanism for *Ps*LSMT.

The emerging importance of the activity of SET domain histone methyltransferases as significant factors in regulating gene expression has spurred intense structural and biochemical interest in this class of PKMTs. *Ps*LSMT, a non-histone PKMT, was the first SET domain PKMT to be sequenced and functionally characterized (*21*, *32*), although the identification of the structurally unique SET domain and its phylogenetic association with histone PKMTs came much later (*33*). The "methylation mark" created by histone PKMTs at site-specific lysyl residues in histones carries information not only according to which lysyl residue is methylated but also according to the degree of methylation (*11*, *34*, *35*). This information has been described as part of the "histone code" which, in conjunction with other covalent modifications such as phosphorylation and acetylation, provides an elegant mechanism for fine-tuning gene expression in response to developmental and tissue-specific signals. Variability in the number of methyl groups transferred by histone methyltransferases is of interest both structurally and mechanistically, and structural studies have identified steric constraints within the active site of the SET domain as being important for the determination of the number of methyl groups transferred (*11*, *23*, *24*, *36*). Mechanistically, multiple-methyl group transfer by SET domain methyltransferases has been proposed to occur through one of two possibilities, distributive or processive in regard to the dissociation, or lack thereof, of the polypeptide substrate between successive methyl group additions. One of the earliest hypotheses derived from structural identification of the SET domain was the unique arrangement of substrate binding sites which would allow for the successive addition of methyl groups without dissociation of the polypeptide substrate (*8*). Indeed, the recent identification of enzymes capable of removing methyl groups from methylated lysyl residues (*37*−*40*), as well as binding proteins with specificity for MeLys, Me_2-Lys, and Me_3Lys residues (*5*, *7*, *41*−*52*), argues that a lack of dissociation of SET domain PKMTs from their respective polypeptide substrates between successive methyl group transfers could have in vivo functional significance. Logically, without the processivity of di- and trimethyltransferases, MeLys and Me_2Lys histone marks, for instance, could be easily modified to Me_2- and/or Me_3Lys, thus potentially inappropriately altering chromatin structure by recruiting different proteins that discriminate among varying degrees of lysine methylation and forming improper complexes. Likewise, if the methyltransferases were distributive enzymes and a methyllysyl binding protein were to dock to the residue prior to formation of the final product, the coding inherent in the methylation status would be compromised. Product specificity changes, such as those which have been implicated in some SET domain PKMTs which reside in multimeric complexes [e.g., ESET/SETDB1 and SET1/MLL (*53*, *54*)], may be modulated by protein partners, and thus, further deconvolution of the enzyme reaction mechanism remains to be elucidated upon in vitro recapitulation of in vivo complexes. In this way, the reaction mechanism is coincident with tight discriminatory substrate requirements and ensures exquisite control of the methylation status of all lysyl residues of the histone tail, adding complexity to strict developmental regulation of PKMT expression patterns.

On the basis of the results reported here, we favor a reaction mechanism for native SET domain PKMTs catalyzing multiple methylations which involves the processive transfer of methyl groups to the target polypeptide substrate without enzyme dissociation. Additionally, we believe that this is reflected by hybrid ping-pong-like double-reciprocal velocity plots which indicate the formation of enzyme complexes between SET domain PKMTs and polypeptide substrates. These studies also emphasize the importance of reaction times during enzymatic activity measurements of SET domain PKMTs which support formation of the final methylated lysyl product during kinetic reaction mechanism studies.

REFERENCES

1. Schultz, J., Milpetz, F., Bork, P., and Ponting, C. P. (1998) SMART, a simple modular architecture research tool: Identification of signaling domains, *Proc. Natl. Acad. Sci. U.S.A. 95*, 5857−5864.

2. Dirk, L. M. A., Trievel, R. C., and Houtz, R. L. (2006) Non-Histone Protein Lysine Methyltransferases: Structure and Catalytic Roles, in *The Enzymes* (Tamanoi, F., and Clarke, S., Eds.) 1st ed., pp 179−229, Elsevier Academic Press, Burlington, MA.
3. Lee, D. Y., Teyssier, C., Strahl, B. D., and Stallcup, M. R. (2005) Role of protein methylation in regulation of transcription, *Endocr. Rev. 26*, 147−170.
4. Xiao, B., Wilson, J. R., and Gamblin, S. J. (2003) SET domains and histone methylation, *Curr. Opin. Struct. Biol. 13*, 699−705.
5. de la Cruz, X., Lois, S., Sanchez-Molina, S., and Martinez-Balbas, M. A. (2005) Do protein motifs read the histone code? *BioEssays 27*, 164−175.
6. Cheng, X., Collins, R. E., and Zhang, X. (2005) Structural and sequence motifs of protein (histone) methylation enzymes, *Annu. Rev. Biophys. Biomol. Struct. 34*, 267−294.
7. Trievel, R. C. (2004) Structure and function of histone methyltransferases, *Crit. Rev. Eukaryotic Gene Expression 14*, 147−169.
8. Trievel, R. C., Beach, B. M., Dirk, L. M., Houtz, R. L., and Hurley, J. H. (2002) Structure and catalytic mechanism of a SET domain protein methyltransferase, *Cell 111*, 91−103.
9. Esteve, P. O., Patnaik, D., Chin, H. G., Benner, J., Teitell, M. A., and Pradhan, S. (2005) Functional analysis of the N- and C-terminus of mammalian G9a histone H3 methyltransferase, *Nucleic Acids Res. 33*, 3211−3223.
10. Patnaik, D., Chin, H. G., Esteve, P. O., Benner, J., Jacobsen, S. E., and Pradhan, S. (2004) Substrate specificity and kinetic mechanism of mammalian G9a histone H3 methyltransferase, *J. Biol. Chem. 279*, 53248−53258.
11. Zhang, X., Yang, Z., Khan, S. I., Horton, J. R., Tamaru, H., Selker, E. U., and Cheng, X. (2003) Structural basis for the product specificity of histone lysine methyltransferases, *Mol. Cell 12*, 177−185.
12. Eskeland, R., Czermin, B., Boeke, J., Bonaldi, T., Regula, J. T., and Imhof, A. (2004) The N-terminus of *Drosophila* SU(VAR)3−9 mediates dimerization and regulates its methyltransferase activity, *Biochemistry 43*, 3740−3749.
13. Chin, H. G., Patnaik, D., Esteve, P. O., Jacobsen, S. E., and Pradhan, S. (2006) Catalytic properties and kinetic mechanism of human recombinant Lys-9 histone H3 methyltransferase SUV39H1: Participation of the chromodomain in enzymatic catalysis, *Biochemistry 45*, 3272−3284.
14. Pesavento, J. J., Mizzen, C. A., and Kelleher, N. L. (2006) Quantitative analysis of modified proteins and their positional isomers by tandem mass spectrometry: Human histone H4, *Anal. Chem. 78*, 4271−4280.
15. Wilkinson, W. R., Gusev, A. I., Proctor, A., Houalla, M., and Hercules, D. M. (1997) Selection of internal standards for quantitative analysis by matrix assisted laser desorption ionization (MALDI) time-of-flight mass spectrometry, *Fresenius J. Anal. Chem. 357*, 241−248.
16. Wang, P., Royer, M., and Houtz, R. L. (1995) Affinity purification of ribulose-1,5-bisphosphate carboxylase/oxygenase large subunit epsilon N-methyltransferase, *Protein Expression Purif. 6*, 528−536.
17. Trievel, R. C., Flynn, E. M., Houtz, R. L., and Hurley, J. H. (2003) Mechanism of multiple lysine methylation by the SET domain enzyme Rubisco LSMT, *Nat. Struct. Biol. 10*, 545−552.
18. Collazo, E., Couture, J. F., Bulfer, S., and Trievel, R. C. (2005) A coupled fluorescent assay for histone methyltransferases, *Anal. Biochem. 342*, 86−92.
19. McCurry, S. D., Gee, R., and Tolbert, N. E. (1982) Ribulose-1,5-bisphosphate carboxylase/oxygenase from spinach, tomato or tobacco leaves, *Methods Enzymol. 90*, 515−521.
20. Chirpich, T. P., Zappia, V., Costilow, R. N., and Barker, H. A. (1970) Lysine 2,3-aminomutase. Purification and properties of a pyridoxal phosphate and S-adenosylmethionine-activated enzyme, *J. Biol. Chem. 245*, 1778−1789.
21. Zheng, Q., Simel, E. J., Klein, P. E., Royer, M. T., and Houtz, R. L. (1998) Expression, purification, and characterization of recombinant ribulose-1,5-bisphosphate carboxylase/oxygenase large subunit epsilon N-methyltransferase, *Protein Expression Purif. 14*, 104−112.
22. Rebouche, C. J., and Broquist, H. P. (1976) Carnitine biosynthesis in *Neurospora crassa*: Enzymatic conversion of lysine to ϵ-N-trimethyllysine, *J. Bacteriol. 126*, 1207−1214.
23. Xiao, B., Jing, C., Wilson, J. R., Walker, P. A., Vasisht, N., Kelly, G., Howell, S., Taylor, I. A., Blackburn, G. M., and Gamblin, S. J. (2003) Structure and catalytic mechanism of the human histone methyltransferase SET7/9, *Nature 421*, 652−656.
24. Qian, C., Wang, X., Manzur, K., Sachchidanand, Farooq, A., Zeng, L., Wang, R., and Zhou, M. M. (2006) Structural insights of the specificity and catalysis of a viral histone H3 lysine 27 methyltransferase, *J. Mol. Biol. 359*, 86−96.
25. Houtz, R. L., Royer, M., and Salvucci, M. E. (1991) Partial purification and characterization of ribulose-1,5-bisphosphate carboxylase/oxygenase large subunit epsilon N-methyltransferase, *Plant Physiol. 97*, 913−920.
26. Durban, E., Nochumson, S., Kim, S., Paik, W. K., and Chan, S. K. (1978) Cytochrome c-specific protein-lysine methyltransferase from *Neurospora crassa*. Purification, characterization, and substrate requirements, *J. Biol. Chem. 253*, 1427−1435.
27. Durban, E., Kim, S., Jun, G.-J., and Paik, W. K. (1983) Cytochrome c specific protein-lysine methyltransferase from *Neurospora crassa*: Kinetic mechanism, *Korean J. Biochem. 15*, 19−24.
28. Xiao, B., Jing, C., Kelly, G., Walker, P. A., Muskett, F. W., Frenkiel, T. A., Martin, S. R., Sarma, K., Reinberg, D., Gamblin, S. J., and Wilson, J. R. (2005) Specificity and mechanism of the histone methyltransferase PR-Set7, *Genes Dev. 19*, 1444−1454.
29. American Chemical Society (2006) *SciFinder Scholar 2006*, American Chemical Society, Washington, DC.
30. Couture, J. F., Hauk, G., Thompson, M. J., Blackburn, G. M., and Trievel, R. C. (2006) Catalytic roles for carbon-oxygen hydrogen bonding in SET domain lysine methyltransferases, *J. Biol. Chem. 281*, 19280−19287.
31. Segel, I. H. (1975) *Enzyme Kinetics: Behavior and Analysis of Rapid Equilibrium and Steady State Enzyme Systems*, Wiley, New York.
32. Klein, R. R., and Houtz, R. L. (1995) Cloning and developmental expression of pea ribulose-1,5-bisphosphate carboxylase/oxygenase large subunit N-methyltransferase, *Plant Mol. Biol. 27*, 249−261.
33. Rea, S., Eisenhaber, F., O'Carroll, D., Strahl, B. D., Sun, Z. W., Schmid, M., Opravil, S., Mechtler, K., Ponting, C. P., Allis, C. D., and Jenuwein, T. (2000) Regulation of chromatin structure by site-specific histone H3 methyltransferases, *Nature 406*, 593−599.
34. Santos-Rosa, H., Schneider, R., Bannister, A. J., Sherriff, J., Bernstein, B. E., Emre, N. C., Schreiber, S. L., Mellor, J., and Kouzarides, T. (2002) Active genes are tri-methylated at K4 of histone H3, *Nature 419*, 407−411.
35. Tamaru, H., Zhang, X., McMillen, D., Singh, P. B., Nakayama, J., Grewal, S. I., Allis, C. D., Cheng, X., and Selker, E. U. (2003) Trimethylated lysine 9 of histone H3 is a mark for DNA methylation in *Neurospora crassa*, *Nat. Genet. 34*, 75−79.
36. Couture, J. F., Collazo, E., Brunzelle, J. S., and Trievel, R. C. (2005) Structural and functional analysis of SET8, a histone H4 Lys-20 methyltransferase, *Genes Dev. 19*, 1455−1465.
37. Shi, Y., Lan, F., Matson, C., Mulligan, P., Whetstine, J. R., Cole, P. A., Casero, R. A., and Shi, Y. (2004) Histone demethylation mediated by the nuclear amine oxidase homolog LSD1, *Cell 119*, 941−953.
38. Tsukada, Y., Fang, J., Erdjument-Bromage, H., Warren, M. E., Borchers, C. H., Tempst, P., and Zhang, Y. (2006) Histone demethylation by a family of JmjC domain-containing proteins, *Nature 439*, 811−816.
39. Shi, Y. J., Matson, C., Lan, F., Iwase, S., Baba, T., and Shi, Y. (2005) Regulation of LSD1 histone demethylase activity by its associated factors, *Mol. Cell 19*, 857−864.
40. Chen, Z., Zang, J., Whetstine, J., Hong, X., Davrazou, F., Kutateladze, T. G., Simpson, M., Mao, Q., Pan, C. H., Dai, S., Hagman, J., Hansen, K., Shi, Y., and Zhang, G. (2006) Structural insights into histone demethylation by JMJD2 family members, *Cell 125*, 691−702.
41. Bannister, A. J., Zegerman, P., Partridge, J. F., Miska, E. A., Thomas, J. O., Allshire, R. C., and Kouzarides, T. (2001) Selective recognition of methylated lysine 9 on histone H3 by the HP1 chromo domain, *Nature 410*, 120−124.
42. Huang, Y., Fang, J., Bedford, M. T., Zhang, Y., and Xu, R. M. (2006) Recognition of histone H3 lysine-4 methylation by the double tudor domain of JMJD2A, *Science 312*, 748−751.
43. Huyen, Y., Zgheib, O., Ditullio, R. A., Jr., Gorgoulis, V. G., Zacharatos, P., Petty, T. J., Sheston, E. A., Mellert, H. S., Stavridi, E. S., and Halazonetis, T. D. (2004) Methylated lysine 79 of histone H3 targets 53BP1 to DNA double-strand breaks, *Nature 432*, 406−411.

44. Kim, J., Daniel, J., Espejo, A., Lake, A., Krishna, M., Xia, L., Zhang, Y., and Bedford, M. T. (2006) Tudor, MBT and chromo domains gauge the degree of lysine methylation, *EMBO Rep. 7*, 397−403.
45. Klymenko, T., Papp, B., Fischle, W., Kocher, T., Schelder, M., Fritsch, C., Wild, B., Wilm, M., and Muller, J. (2006) A Polycomb group protein complex with sequence-specific DNA-binding and selective methyl-lysine-binding activities, *Genes Dev. 20*, 1110−1122.
46. Lachner, M., O'Carroll, D., Rea, S., Mechtler, K., and Jenuwein, T. (2001) Methylation of histone H3 lysine 9 creates a binding site for HP1 proteins, *Nature 410*, 116−120.
47. Li, H., Ilin, S., Wang, W., Duncan, E. M., Wysocka, J., Allis, C. D., and Patel, D. J. (2006) Molecular basis for site-specific read-out of histone H3K4me3 by the BPTF PHD finger of NURF, *Nature 442*, 91−95.
48. Pena, P. V., Davrazou, F., Shi, X., Walter, K. L., Verkhusha, V. V., Gozani, O., Zhao, R., and Kutateladze, T. G. (2006) Molecular mechanism of histone H3K4me3 recognition by plant homeodomain of ING2, *Nature 442*, 100−103.
49. Ramos, A., Hollingworth, D., Adinolfi, S., Castets, M., Kelly, G., Frenkiel, T. A., Bardoni, B., and Pastore, A. (2006) The structure of the N-terminal domain of the fragile X mental retardation protein: A platform for protein-protein interaction, *Structure 14*, 21−31.
50. Shi, X., Hong, T., Walter, K. L., Ewalt, M., Michishita, E., Hung, T., Carney, D., Pena, P., Lan, F., Kaadige, M. R., Lacoste, N., Cayrou, C., Davrazou, F., Saha, A., Cairns, B. R., Ayer, D. E., Kutateladze, T. G., Shi, Y., Cote, J., Chua, K. F., and Gozani, O. (2006) ING2 PHD domain links histone H3 lysine 4 methylation to active gene repression, *Nature 442*, 96−99.
51. Sims, R. J., III, Chen, C. F., Santos-Rosa, H., Kouzarides, T., Patel, S. S., and Reinberg, D. (2005) Human but not yeast CHD1 binds directly and selectively to histone H3 methylated at lysine 4 via its tandem chromodomains, *J. Biol. Chem. 280*, 41789−41792.
52. Wysocka, J., Swigut, T., Xiao, H., Milne, T. A., Kwon, S. Y., Landry, J., Kauer, M., Tackett, A. J., Chait, B. T., Badenhorst, P., Wu, C., and Allis, C. D. (2006) A PHD finger of NURF couples histone H3 lysine 4 trimethylation with chromatin remodelling, *Nature 442*, 86−90.
53. Wang, H., An, W., Cao, R., Xia, L., Erdjument-Bromage, H., Chatton, B., Tempst, P., Roeder, R. G., and Zhang, Y. (2003) mAM facilitates conversion by ESET of dimethyl to trimethyl lysine 9 of histone H3 to cause transcriptional repression, *Mol. Cell 12*, 475−487.
54. Steward, M. M., Lee, J. S., O'Donovan, A., Wyatt, M., Bernstein, B. E., and Shilatifard, A. (2006) Molecular regulation of H3K4 trimethylation by ASH2L, a shared subunit of MLL complexes, *Nat. Struct. Mol. Biol. 13*, 852−854.

BI6023644